Advances in Computational Design, *Vol. 4, No. 3 (2019) 273-294*
DOI: https://doi.org/10.12989/acd.2019.4.3.273

Optimal design for the reinforced concrete circular isolated footings

Sandra López-Chavarría[a], Arnulfo Luévanos-Rojas[*], Manuel Medina-Elizondo[b], Ricardo Sandoval-Rivas[c] and Francisco Velázquez-Santillán[d]

Department of Civil Engineering, Korean Advanced Institute for Science and Technology, 291 Daehak-ro, Yuseong-gu, Daejeon 305-701, Republic of Korea

(Received January 25, 2019, Revised May 20, 2019, Accepted May 31, 2019)

Abstract. In this paper is presented the minimum cost (optimal design) for reinforced concrete circular isolated footings based on an analytic model. This model considers a load and two moments in directions of the X and Y axes, and the pressure has a variation linear, these are the effects that act on the footing. The minimum cost (optimal design) and the Maple program are shown in Flowcharts. Two numerical experiments are shown to obtain the minimum cost design of the two materials that are used for a circular footing supporting an axial load and moments in two directions in accordance to the code of the ACI (American Concrete Institute), and it is compared against the current design (uniform pressure). Also, the same examples are developed through the normal procedure to verify the minimum cost (optimal design) presented in this document, i.e., the equations of moment, bending shear and punching shear are used to check the thickness, and after, the steel areas of the footing are obtained, and it is compared against the current design (uniform pressure). Results section show that the optimal design is more accurate and more economical than to any other model. Therefore, it is concluded that the optimized design model presented in this paper should be used to obtain the minimum cost design for the circular isolated footings.

Keywords: optimal design; reinforced concrete circular isolated footings; minimum cost design; moments; bending shear; punching shear

1. Introduction

The footings sizes are mostly governed by the axial load and the moments, allowable soil pressure, concrete unit weight, soil unit weight, and the depth of the footing base below the final grade (Al-Ansari 2013, Luévanos-Rojas *et al.* 2017a).

The design for the shallow footing solution is made for the following cases of load applied to the footings: 1) Concentric load, 2) Concentric load and moment around of an axis (X or Y) (uniaxial bending), 3) Concentric load and moment around of two axes (X and Y) (biaxial bending).

∗Corresponding author, Ph.D., E-mail: arnulfol_2007@hotmail.com
[a] Ph.D., E-mail: sandylopez5@hotmail.com
[b] Ph.D., E-mail: drmanuelmedina@yahoo.com.mx
[c] Ph.D. Student, E-mail: ricardo_sandoval_rivas@hotmail.com
[d] Ph.D. Student, E-mail: frankv2010@hotmail.com

http://www.techno-press.org/?journal=acd&subpage=7 ISSN: 2383-8477 (Print), 2466-0523 (Online)

The objective of a designer is to generate an "optimal solution" for the structures design some considerations. An optimal solution usually involves the most economical structure without harming the functional purposes of the structure (Bhalchandra and Adsul 2012).

The optimal design of structures in the last decade has been the topic of many studies in the field of structural design (see Table 1).

The main studies published in the last decade in the topic for the structural foundations optimal design (see Table 2).

Several papers show the mathematical equations to obtain the design of footings are: Design of rectangular isolated footings by Luévanos-Rojas *et al.* (2013); Design of circular isolated footings by Luévanos-Rojas (2014a); Design of rectangular boundary combined footings by Luévanos-Rojas (2014b); Design of trapezoidal boundary combined footings by Luévanos-Rojas (2015); A comparative study for the design of rectangular and circular isolated footings by Luévanos-Rojas (2016b); Design for the rectangular combined footings restricted in two opposite sides by Luévanos-Rojas (2016c); Design of square isolated footings for general case by López-Chavarría *et al.* (2017c); A comparative study for design of trapezoidal and rectangular boundary combined footings by Luévanos-Rojas *et al.* (2017b); Design for the T-shaped combined footings by Luévanos-Rojas *et al.* (2018c); Design for the strap combined footings by Yáñez-Palafox *et al.* (2019b). These papers show only the design equations and same numerical examples for the footings, but the optimal design does not appear.

Thus, there is not paper on the topic with the level of current knowledge on the optimal structural design for the reinforced concrete circular isolated footings. Finally, there are also no elaborate recommendations for the geotechnical and structural design of reinforced concrete circular isolated footings tending the minimum design cost.

This paper presents the optimal design for the circular isolated footings using a new model. This analytical model estimated the minimum cost with constant parameters and decision variables (design variables). The Flowcharts are presented for the minimum cost (optimal design) and for the Maple program. Two numerical examples are presented to estimate the materials cost of the circular footing that support to an axial load, moment around of the "X" axis and moment around of the "Y" axis in accordance with the requirements of the construction code for structural concrete (ACI 318S-14 2014), and it is compared against the current design (uniform pressure). Also, the same examples using the equations of moments, bending shear and punching shear are obtained to verify the thickness, and after, the reinforced steel areas of the footing are obtained, and it is compared against the current design to observe the differences.

2. Methodology

2.1 Model to obtain the radius of circular footings

Fig. 1 shows a circular isolated footing under the application of an axial load and moments in two directions (biaxial bending), where the pressure is different throughout the contact surface.

The radius "*R*" is obtained by the following equations (Luévanos-Rojas 2012):

$$R = \frac{4\sqrt{M_x{}^2 + M_y{}^2}}{P} \tag{1}$$

Table 1 Optimal design of structures

Authors	Main contribution
Aschheim *et al.* (2008)	Optimal design for reinforced concrete beam, column, and wall sections
Yousif *et al.* (2010)	Design optimized for the singly and doubly reinforced concrete rectangular beam sections by the artificial neural networks
Bordignon and Kripka (2012)	Optimal design for the reinforced concrete columns under uniaxial bending compression
Bhalchandra and Adsul (2012)	Optimal cost for a doubly reinforced rectangular beam section
Kaveh and Talatahari (2012)	Design optimized of structures by the hybrid CSS and PSO algorithms
Fleith de Medeiros and Kripka (2013)	Optimal structures to obtain the pre-dimensioning parameters for beams in reinforced concrete buildings
Ozturk and Durmus (2013)	Optimal cost design of reinforced concrete columns by the artificial bee colony algorithm
Awad (2013)	Sandwich beam optimal design using the analytical and numerical solutions
Kripka and Chamberlain Pravia (2013)	Cold-formed steel channel optimal columns by the simulated annealing method
Kaveh *et al*. (2013)	Optimal design for the reinforced concrete retaining walls by the multi-objective genetic algorithm
Shayanfar *et al*. (2013)	Modal load optimal pattern for the building structures pushover analysis
Nascimbene (2013)	Optimal and analysis design of structures composite reinforced with fiber
Tiliouine and Fedghouche (2014)	Optimal cost for the reinforced high strength concrete T-sections under bending
Kao and Yeh (2014a)	Optimal design for the reinforced concrete plane frames by the artificial neural networks
Kao and Yeh (2014b)	Optimal design for the plane frame structures by the artificial neural networks and ratio variables
Abbasnia *et al*. (2014)	Optimal design based in reliability of structural systems using the hybrid genetic algorithm
Kaveh and Mahdavi (2016)	Design optimized for truss structures by a optimization algorithm based on a global sensitivity analysis
Luévanos-Rojas (2016a)	Design optimized for the reinforced concrete rectangular beams of singly reinforced sections with numerical experiments
Gao *et al*. (2017)	A multi-parameter optimal technique in cable-stayed bridges of prestressed concrete considering the prestress in girder
Errouane *et al*. (2017)	Optimal design of probability analysis for fatigue crack in aluminum plate repaired by a bonded composite patch
Gharehbaghi (2018)	Optimal seismic design controlling the damage of the reinforced concrete structures
Hwang *et al.* (2018)	Experimental validation of FE model updating based on multi-objective optimization using the surrogate model
Kaveh and Bijari (2018)	Optimization, simultaneous analysis and design of trusses by the force method
Zhang *et al.* (2018)	Comparison of the performance for shear walls with openings designed by the genetic evolutionary structural optimization methods and elastic stress
Luévanos-Rojas *et al.* (2018a)	Optimization of reinforced concrete beams for rectangular sections with numerical experiments

$$\sigma_{max}\pi R^3 - PR - 4\sqrt{{M_x}^2 + {M_y}^2} = 0 \tag{2}$$

where: the value of "*R*" for Eq. (1) is obtained for when the soil pressure is equal to zero and the value of "*R*" for Eq. (2) is found for when the soil pressure is equal to the soil available allowable

Table 2 Optimal design of foundations structures

Authors	Main contribution
Wang and Kulhawy (2008)	Economic design optimization of foundation
Wang (2009)	Optimal economic design based in reliability of the spread foundation
Rizwan *et al*. (2012)	Optimal cost for the combined footings by the modified complex method of box
Al-Ansari (2013)	Structural optimal cost for the reinforced concrete isolated footing
Al-Ansari (2014)	Footing cost in shape paraboloid of reinforced concrete
Khajehzadeh *et al*. (2014)	Optimal foundation by multi-objective using a global-local gravitational search algorithm
Luévanos-Rojas *et al*. (2017a)	Design optimized for the rectangular isolated footings considering the real soil pressure
Authors	Main contribution
López-Chavarría *et al*. (2017a)	Optimal dimensioning for the square isolated footings: general case
López-Chavarría *et al*. (2017b)	Optimal dimensioning for the corner combined footings
Velázquez-Santillán *et al*. (2018)	Design optimized for the reinforced concrete rectangular combined footings with numerical experiments
Luévanos-Rojas *et al*. (2018b)	Optimal dimensioning for the T-shaped combined footings
Aguilera-Mancilla *et al*. (2019a)	Optimal dimensioning for the strap combined footings

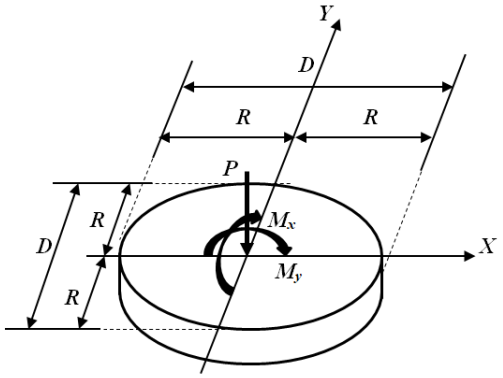

Fig. 1 Circular isolated footing

load capacity "σ_{max}", and the greater values is taken to satisfy the two conditions, because the pressure generated by the footing must be greater than or equal to zero and less or equal to the soil available allowable load capacity (Luévanos-Rojas 2012).

The soil available allowable load capacity "σ_{max}" is (Luévanos-Rojas 2014a):

$$\sigma_{max} = q_a - \gamma_{ppz} - \gamma_{pps} \tag{3}$$

where: q_a is the soil allowable load capacity, γ_{ppz} is the footing weight in square meters, γ_{pps} is the soil fill weight in square meters.

If the earthquake loads and/or the wind are considered in the design, then the soil allowable load capacity must be increased by 33% (ACI 318S-14 2014).

Also Eq. (3) could be presented as follows:

$$\sigma_{max} = q_a - \gamma_c(d + r) - \gamma_g(H - d - r) \tag{4}$$

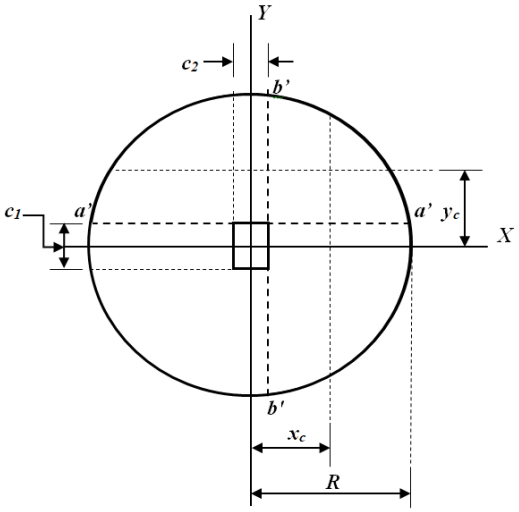

Fig. 2 Critical sections for moments

where: γ_c is the concrete density = 24 kN/m^3, γ_g is the soil density, d is the effective depth of the footing (effective cant), r is the concrete coating in the footing and H is the depth of the footing base below the final grade.

2.2 Model to obtain the design of circular footings

The requirements of the construction code for the footings that support to a column, the critical sections are (ACI 318S-14 2014): The maximum moment is presented in face of column; Bending shear is located at a distance "*d*"; Punching shear is found in the perimeter "b_o" (this perimeter is localized at a distance of "*d/2*" from face of column in both direction).

2.2.1 Moments

The critical sections for moments are located on the *a'- a'* and *b'-b'* axes (see Fig. 2)
The moment "$M_{a'-a'}$" that acts around the "*a'-a'*" axis is (Luévanos-Rojas 2014a, 2016b):

$$M_{a'-a'} = \left[\frac{P_u(c_1{}^2 + 8R^2)}{24\pi R^2} + \frac{M_{ux}c_1(c_1{}^2 - 10R^2)}{24\pi R^4}\right]\sqrt{4R^2 - c_1{}^2} + \frac{(2M_{ux} - P_u c_1)\left[\pi - 2\,Asin\left(\frac{c_1}{2R}\right)\right]}{4\pi} \tag{5}$$

The moment "$M_{b'-b'}$" that acts around the "*b'-b'*" axis is (Luévanos-Rojas 2014, 2016):

$$M_{b'-b'} = \left[\frac{P_u(c_2{}^2 + 8R^2)}{24\pi R^2} + \frac{M_{uy}c_2(c_2{}^2 - 10R^2)}{24\pi R^4}\right]\sqrt{4R^2 - c_2{}^2} + \frac{(2M_{uy} - P_u c_2)\left[\pi - 2\,Asin\left(\frac{c_2}{2R}\right)\right]}{4\pi} \tag{6}$$

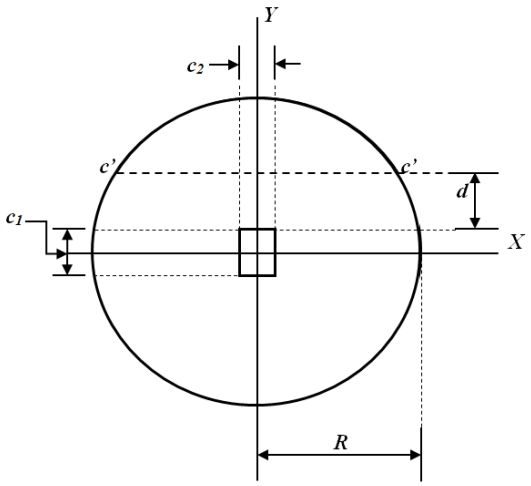

Fig. 3 Critical section for bending shear

2.2.2 Bending shear

The critical section for bending shear (unidirectional shear force) is located on the *c'- c'* axis (see Fig. 3).

The bending shear that acts "V_f" is (Luévanos-Rojas 2014a, 2016b):

$$V_f = P_u\left[\frac{1}{2}-\left(\frac{c_1+2d}{4\pi R^2}\right)\sqrt{4R^2-(c_1+2d)^2}-\frac{1}{\pi}Asin\left(\frac{c_1+2d}{2R}\right)\right] + \frac{M_{ux}[4R^2-(c_1+2d)^2]^{3/2}}{3\pi R^4} \tag{7}$$

2.2.3 Punching shear

The critical section for punching shear (bidirectional shear force) is located on rectangular surface formed by the corners 5, 6, 7 and 8, (see Fig. 4).

The punching shear that acts "V_p" is (Luévanos-Rojas 2014a, 2016b):

$$V_P = \frac{P_u[\pi R^2-(c_1+d)(c_2+d)]}{\pi R^2} \tag{8}$$

The equations proposed by the ACI code are shown in the appendix.

2.3 Objective function to minimize the cost

A cost function is defined as the total minimum cost "C_{tm}" which is equal to steel cost more the concrete cost. These costs include the material costs and the manpower costs, respectively. The cost of the circular isolated footing is:

$$C_{tm} = V_c C_c + V_s \gamma_s C_s \tag{9}$$

where: C_c is cost of concrete for 1 m^3 in dollars, C_s is cost of steel for 1 kN of steel in dollars, V_s is volume of steel, V_c is volume of concrete and γ_s is steel density = 76.94 kN/m^3.

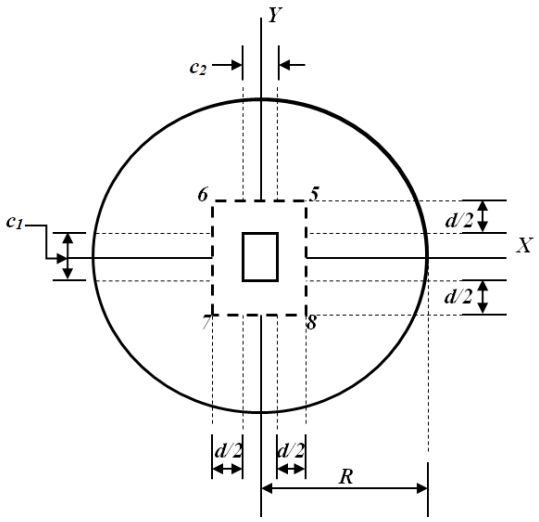

Fig. 4 Critical section for punching shear

The amount of steel is estimated as follows: The footing will be reinforced in the form of a rectangular or square grid and a circular ring at a distance *r* cm from the outer edge of the footing.

The reinforcing area "A_{sx}" and "A_{sy}" in the direction "*X*" and "*Y*" are given as:

$$A_{sx} = \rho_x b_{wy} d;\ A_{sy} = \rho_y b_{wx} d \tag{10}$$

where: ρ_x is the ratio of the steel in the direction of the "X" axis, ρ_y is the ratio of the steel in the direction of the "Y" axis.

The number of rods "n_x" and "n_y" in the two directions is obtained as follows:

$$n_x = \frac{A_{sx}}{a_s};\ n_y = \frac{A_{sy}}{a_s} \tag{11}$$

where: a_s is the area of the rod that is used and this is considered the same in both directions.

The separation for reinforcing steel in both directions is:

$$s_x = \frac{b_{wy} a_s}{A_{sx}};\ s_y = \frac{b_{wx} a_s}{A_{sy}} \tag{12}$$

The length of the steel bars in the directions "X" and "Y" are:

$$L_x = 2R + 4 \sum_{j=1}^{(n_x-3)/2} \sqrt{R^2 - (j s_x)^2} \tag{13}$$

$$L_y = 2R + 4 \sum_{i=1}^{(n_y-3)/2} \sqrt{R^2 - \left(i s_y\right)^2} \tag{14}$$

The length of the circumferential reinforcing steel is calculated as:

$$L_c = 2\pi(R - r) \tag{15}$$

The total volume of reinforcing steel for the circular footing is:

$$V_s = a_s\left(L_y + L_x + L_c\right) \tag{16}$$

The volume of concrete for the circular footing is:

$$V_c = \pi R^2 t - a_s\left(L_y + L_x + L_c\right) \tag{17}$$

Substituting the Eqs. (16) and (17) into Eq. (9) is obtained:

$$C_{tm} = C_c\left[\pi R^2 t - a_s\left(L_y + L_x + L_c\right)\right] + \gamma_s C_s\left[a_s\left(L_y + L_x + L_c\right)\right] \tag{18}$$

Now, considering $\alpha = \gamma_s C_s / C_c$, and substituting into Eq. (18) is found:

$$C_{tm} = C_c\left[\pi R^2 t - a_s\left(L_y + L_x + L_c\right)(1-\alpha)\right] \tag{19}$$

Substituting the Eqs. (13), (14) and (15) into Eq. (19) is obtained:

$$C_{tm} = \left[\begin{pmatrix} 4R + 4\sum_{i=1}^{\frac{(n_y-3)}{2}} \sqrt{R^2 - \left(is_y\right)^2} + \\ 4\sum_{j=1}^{(n_x-3)/2} \sqrt{R^2 - (js_x)^2} + 2\pi(R-r) \end{pmatrix}(\alpha - 1)a_s + \pi R^2 t\right] C_c \tag{20}$$

2.4 Constraint functions

Equations of the model for the dimensioning of circular isolated footings, the new model for the design of the circular isolated footings, and the construction code requirements for concrete are considered to obtain the constraint functions:

$$R \geq \frac{4\sqrt{{M_x}^2 + {M_y}^2}}{P} \tag{21}$$

$$\left[q_a - \gamma_c(d+r) - \gamma_g(H-d-r)\right]\pi R^3 - PR - 4\sqrt{{M_x}^2 + {M_y}^2} \geq 0 \tag{22}$$

$$\left[\frac{P_u({c_1}^2 + 8R^2)}{24\pi R^2} + \frac{M_{ux}c_1({c_1}^2 - 10R^2)}{24\pi R^4}\right]\sqrt{4R^2 - {c_1}^2} + \frac{(2M_{ux} - P_u c_1)\left[\pi - 2\,Asin\left(\frac{c_1}{2R}\right)\right]}{4\pi} \leq \emptyset_f f_y \rho_y \sqrt{4R^2 - {c_1}^2} d^2\left(1 - \frac{0.59\rho_y f_y}{f'_c}\right) \tag{23}$$

$$\left[\frac{P_u({c_2}^2 + 8R^2)}{24\pi R^2} + \frac{M_{uy}c_2({c_2}^2 - 10R^2)}{24\pi R^4}\right]\sqrt{4R^2 - {c_2}^2} + \frac{(2M_{uy} - P_u c_2)\left[\pi - 2\,Asin\left(\frac{c_2}{2R}\right)\right]}{4\pi} \leq \emptyset_f f_y \rho_x \sqrt{4R^2 - {c_2}^2} d^2\left(1 - \frac{0.59\rho_x f_y}{f'_c}\right) \tag{24}$$

$$P_u\left[\frac{1}{2}-\left(\frac{c_1+2d}{4\pi R^2}\right)\sqrt{4R^2-(c_1+2d)^2}-\frac{1}{\pi}Asin\left(\frac{c_1+2d}{2R}\right)\right] + \frac{M_{ux}[4R^2-(c_1+2d)^2]^{3/2}}{3\pi R^4} \leq 0.17\emptyset_v\sqrt{f'_c}\sqrt{4R^2-(c_1+2d)^2}d \tag{25}$$

$$\frac{P_u[\pi R^2-(c_1+d)(c_2+d)]}{\pi R^2} \leq \begin{cases} 0.17\emptyset_v\left(1+\frac{2}{\beta_c}\right)\sqrt{f'_c}[2(c_1+c_2+2d)]d \\ 0.083\emptyset_v\left(\frac{\alpha_s d}{b_0}+2\right)\sqrt{f'_c}[2(c_1+c_2+2d)]d \\ 0.33\emptyset_v\sqrt{f'_c}[2(c_1+c_2+2d)]d \end{cases} \tag{26}$$

$$\rho_y,\rho_x \leq 0.75\left[\frac{0.85\beta_1 f'_c}{f_y}\left(\frac{600}{600+f_y}\right)\right] \tag{27}$$

$$\rho_y,\rho_x \geq \begin{cases} \frac{0.25\sqrt{f'_c}}{f_y} \\ \frac{1.4}{f_y} \end{cases} \tag{28}$$

$$A_{sy}=\rho_y\sqrt{4R^2-{c_1}^2}d \tag{29}$$

$$A_{sx}=\rho_x\sqrt{4R^2-{c_2}^2}d \tag{30}$$

$$n_x=\frac{A_{sx}}{a_s} \tag{31}$$

$$n_y=\frac{A_{sy}}{a_s} \tag{32}$$

$$s_x=\frac{\sqrt{4R^2-{c_2}^2}a_s}{A_{sx}} \tag{33}$$

$$s_y=\frac{\sqrt{4R^2-{c_1}^2}a_s}{A_{sy}} \tag{34}$$

It is assumed that all variables are non-negative.

Fig. 5 shows the flowchart of the algorithm for the reinforced concrete circular isolated footing optimal design.

Fig. 6 shows the flowchart of Maple program for the reinforced concrete circular isolated footing optimal design.

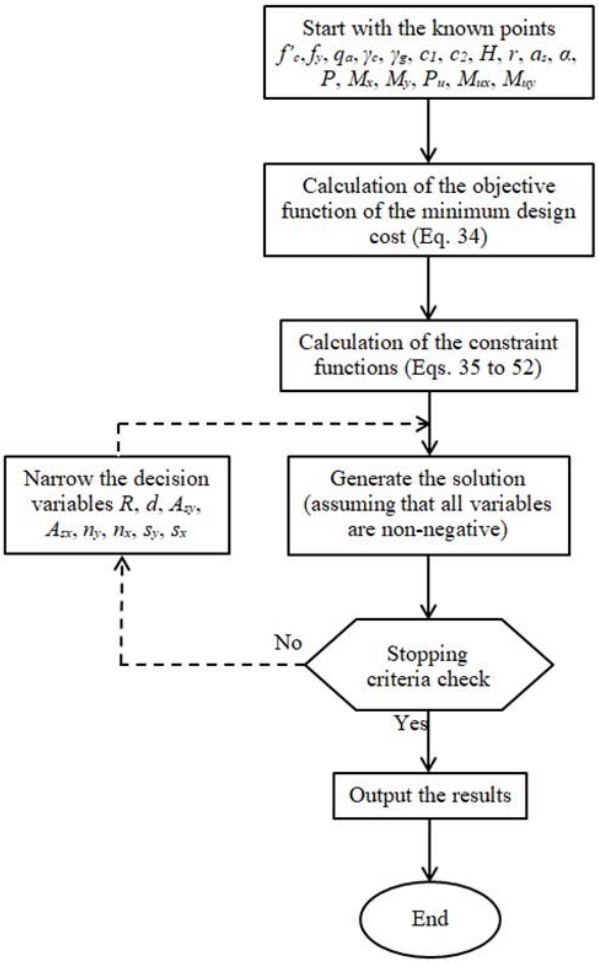

Fig. 5 Flowchart of the optimal design model

3. Numerical problem

Design of two reinforced concrete circular isolated footing supporting a square column with the information following is presented: $f'_c = 21$ *MPa*, $f_y = 420$ *MPa*, $q_a = 220$ *kN/m*^{2}, $\gamma_c = 24$ *kN/m*^{3}, $\gamma_g = 15$ *kN/m*^{3}, $c_1 = 40$ *cm*, $c_2 = 40$ *cm*, $H = 1.5$ *m*, $r = 8$ *cm*, $a_s = 1.98$ *cm*^{2}, $\alpha = 90$. The forces and moments that act for each case on the footing are: Case 1; $P_D = 700$ *kN*, $P_L = 500$ *kN*, $M_{Dx} = 240$ *kN-m*, $M_{Lx} = 160$ *kN-m*, $M_{Dy} = 120$ *kN-m*, $M_{Ly} = 80$ *kN-m*. Case 2; $P_D = 700$ *kN*, $P_L = 500$ *kN*, $M_{Dx} = 140$ *kN-m*, $M_{Lx} = 100$ *kN-m*, $M_{Dy} = 120$ *kN-m*, $M_{Ly} = 80$ *kN-m*. It is required to determine the values of the optimal relations of reinforcing steel ρ_x and ρ_y, the optimal areas of reinforcing steel A_{sx} and A_{sy}, the number of rods n_x and n_y, the separation of reinforcing steel s_x and s_y, the optimum radius of the footing R, and the optimal effective depth of the concrete d.

Where: P_D is the dead load, P_L is the live load, M_{Dx} is the moment of the dead load around the "X-X" axis, M_{Lx} is the moment of the live load around the "X-X" axis, M_{Dy} is the moment of the dead load around the "Y-Y" axis, M_{Ly} is the moment of the live load around the "Y-Y" axis.

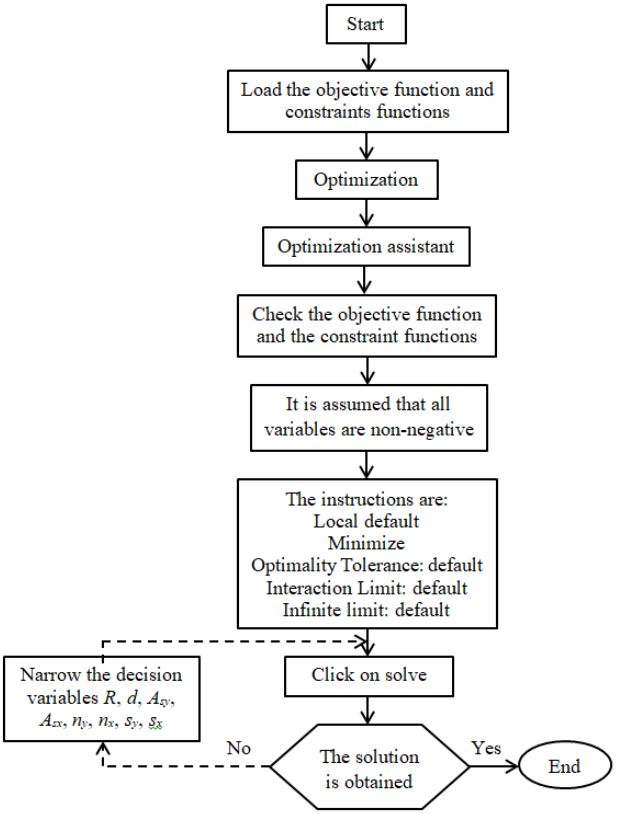

Fig. 6 Flowchart of Maple program

The loads and moments that act on the footing are: Case 1; $P = 1200$ *kN*, $M_x = 400$ *kN-m*, $M_y = 200$ *kN-m*. Case 2; $P = 1200$ *kN*, $M_x = 240$ *kN-m*, $M_y = 200$ *kN-m*.

The loads and moments that act on the footing are factored by Eq. (44): Case 1; $P_u = 1640$ *kN*, $M_{ux} = 544$ *kN-m*, $M_{uy} = 272$ *kN-m*. Case 2; $P_u = 1640$ *kN*, $M_{ux} = 328$ *kN-m*, $M_{uy} = 272$ *kN-m*.

Substituting the values that correspond into Eq. (20) to find the objective function and also into Eqs. (21) to (34) to obtain the constraint functions for each case.

In order to evaluate the optimal design with respect to the minimum cost for the reinforced concrete isolated footing in a circular shape for the new model, the MAPLE15 software is used to obtain the optimization problem solution.

Table 3 shows the effective depth "*d*" varying its value of 38.43, 42.00, 47.00, 52.00, 57.00 and 62.00 *cm* for the case 1, and for the case 2 varies its value of 38.43, 42.00, 47.00, 52.00, 57.00 and 62.00 *cm*. Table 4 presents the radius "*R*" of the footing changing its value of 188.18, 190.00, 200.00, 210.00, 220.00 and 230.00 *cm* for the case 1, and for the case 2 changes its value of 177.18, 180.00, 190.00, 200.00, 210.00 and 220.00 *cm*. Table 5 shows the percentage of reinforcing steel in the direction "Y" axis "ρ_y" modifying the value of 0.00500, 0.00450, 0.00400, 0.00363, 0.00350 and 0.000333 for the case 1, and for the case 2 modifies its value of 0.00500, 0.00450, 0.00400, 0.00350, 0.00336 and 0.000333. The results of the optimal design for the reinforced concrete circular isolated footing are marked on the tables and these provide a very precise estimate of the minimum design cost of the materials.

Table 3 Effective depth "d" varies

R (cm)	d (cm)	ρ_y	A_{sy} (cm^2)	n_y	s_y (cm)	ρ_x	A_{sx} (cm^2)	n_x	s_x (cm)	C_{tm} ($)
Case 1										
188.18	**38.43**	**0.00363**	**52.16**	**26.34**	**14.21**	**0.00333**	**47.93**	**24.21**	**15.46**	**7.859C$_c$**
188.31	42.00	0.00333	52.43	26.48	14.14	0.00333	52.43	26.48	14.14	8.382C$_c$
188.49	47.00	0.00333	58.72	29.66	12.64	0.00333	58.72	29.66	12.64	9.344C$_c$
188.67	52.00	0.00333	65.04	32.85	11.42	0.00333	65.04	32.85	11.42	10.186C$_c$
188.85	57.00	0.00333	71.36	36.04	10.42	0.00333	71.36	36.04	10.42	11.152C$_c$
189.03	62.00	0.00333	77.69	39.24	9.58	0.00333	77.69	39.24	9.58	12.112C_c
Case 2										
177.18	**38.24**	**0.00336**	**45.19**	**22.82**	**15.43**	**0.00336**	**45.19**	**22.82**	**15.43**	**6.812C$_c$**
177.25	42.00	0.00333	49.31	24.91	14.14	0.00333	49.31	24.91	14.14	7.395C$_c$
177.43	47.00	0.00333	55.24	27.90	12.64	0.00333	55.24	27.90	12.64	8.267C$_c$
177.60	52.00	0.00333	61.18	30.90	11.42	0.00333	61.18	30.90	11.42	9.019C$_c$
177.78	57.00	0.00333	67.13	33.90	10.42	0.00333	67.13	33.90	10.42	9.890C$_c$
177.96	62.00	0.00333	73.09	36.92	9.58	0.00333	73.09	36.92	9.58	12.112C_c

Table 4 Radius "R" is modified

R (cm)	d (cm)	ρ_y	A_{sy} (cm^2)	n_y	s_y (cm)	ρ_x	A_{sx} (cm^2)	n_x	s_x (cm)	C_{tm} ($)
Case 1										
188.18	**38.43**	**0.00363**	**52.16**	**26.34**	**14.21**	**0.00333**	**47.93**	**24.21**	**15.46**	**7.859C$_c$**
190.00	38.46	0.00362	52.59	26.56	14.23	0.00333	48.44	24.47	15.44	7.999C$_c$
200.00	38.60	0.00358	54.99	27.78	14.33	0.00333	51.21	25.86	15.39	8.926C$_c$
210.00	38.72	0.00355	57.40	28.99	14.42	0.00333	53.96	27.25	15.34	9.827C$_c$
220.00	38.82	0.00352	59.82	30.21	14.50	0.00333	56.70	28.64	15.30	10.776C$_c$
230.00	38.91	0.00349	62.22	31.43	14.58	0.00333	59.44	30.02	15.27	11.838C$_c$
Case 2										
177.18	**38.24**	**0.00336**	**45.19**	**22.82**	**15.43**	**0.00336**	**45.19**	**22.82**	**15.43**	**6.812C$_c$**
180.00	38.30	0.00333	45.67	23.07	15.51	0.00333	45.67	23.07	15.51	7.137C$_c$
190.00	38.45	0.00333	48.43	24.46	15.45	0.00333	48.43	24.46	15.45	7.888C$_c$
200.00	38.59	0.00333	51.20	25.86	15.39	0.00333	51.20	25.86	15.39	8.813C$_c$
210.00	38.71	0.00333	53.95	27.25	15.34	0.00333	53.95	27.25	15.34	9.782C$_c$
220.00	38.82	0.00333	56.70	28.64	15.30	0.00333	56.70	28.64	15.30	10.662C$_c$

4. Results

Table 3 shows the results for the numerical examples by varying the effective depth "*d*". When the value of "*d*" is increased: For the case 1, the value of "ρ_x" is constant of 0.00333, the value of "ρ_y" decreases starting from 0.00363 until reaching 0.00333 (minimum percentage), and the values of "A_{sy}", "A_{sx}", "R" and "C_{tm}" increase. For the case 2, the values of "ρ_x" and "ρ_y" decrease starting

Table 5 Percentage of reinforcing steel "ρ_y" changes

R (cm)	d (cm)	ρ_y	A_{sy} (cm^2)	n_y	s_y (cm)	ρ_x	A_{sx} (cm^2)	n_x	s_x (cm)	C_{tm} ($)
Case 1										
188.18	38.42	0.00500	71.89	36.31	10.31	0.00333	47.93	24.21	15.46	8.391C_c
188.18	38.42	0.00450	64.71	32.68	11.45	0.00333	47.93	24.21	15.46	8.187C_c
188.18	38.42	0.00400	57.52	29.05	12.88	0.00333	47.93	24.21	15.46	8.041C_c
188.18	**38.43**	**0.00363**	**52.16**	**26.34**	**14.21**	**0.00333**	**47.93**	**24.21**	**15.46**	**7.859C_c**
188.20	39.11	0.00350	51.23	25.87	14.47	0.00333	48.79	24.64	15.19	7.935C_c
188.23	40.02	0.00333	49.94	25.22	14.84	0.00333	49.94	25.22	14.84	8.101C_c
Case 2										
177.12	38.24	0.00500	67.30	33.99	10.36	0.00333	44.86	22.66	15.53	7.394C_c
177.12	38.24	0.00450	60.56	30.59	11.51	0.00333	44.86	22.66	15.53	7.206C_c
177.12	38.24	0.00400	53.84	27.18	12.95	0.00333	44.86	22.66	15.53	7.075C_c
177.12	38.24	0.00350	47.11	22.79	14.79	0.00333	44.86	22.66	15.53	6.888C_c
177.18	**38.24**	**0.00336**	**45.19**	**22.82**	**15.43**	**0.00336**	**45.19**	**22.82**	**15.43**	**6.812C_c**
177.13	38.41	0.00333	45.07	22.76	15.47	0.00333	45.07	22.76	15.47	6.823C_c

from 0.00336 until reaching 0.00333 (minimum percentage), and the values of "A_{sy}", "A_{sx}", "R" and "C_{tm}" increase.

Table 4 shows the results for the numerical examples by modifying the radius "R" of the footing. When the value of "R" is increased: For the case 1, the value of "ρ_x" is constant of 0.00333, the value of "ρ_y" decreases starting from 0.00363 until reaching 0.00333 (minimum percentage), and the values of "A_{sy}", "A_{sx}", "d" and "C_{tm}" increase. For the case 2, the values of "ρ_x" and "ρ_y" decrease starting from 0.00336 until reaching 0.00333 (minimum percentage), and the values of "A_{sy}", "A_{sx}", "d" and "C_{tm}" increase.

Table 5 shows the results for the numerical examples by varying the steel reinforcement percentage "ρ_y" from 0.00500 to 0.00333 (minimum percentage). When the value of "ρ_y" is reduced: For the case 1, the value of "ρ_x" is constant of 0.00333, the values of "R", "A_{sx}" and "d" are increased, the value of "A_{sy}" is reduced, and the "C_{tm}" is reduced until percentage of ρ_y = 0.00363 and subsequently increases. For the case 2, the value of "ρ_x" is constant of 0.00333 with exception of the value of ρ_x = 0.00336 (value that presents the minimum cost), the value of "R" is constant with exception of the value that presents the minimum cost, the value of "d" is constant with exception of the value of ρ_y = 0.00333 that presents the minimum percentage, the value of "A_{sx}" increases until steel area of $A_{sx} = 45.19\ cm^2$ that presents the minimum cost and subsequently reduces, the value of "A_{sy}" is reduced, and the "C_{tm}" is reduced until percentage of ρ_y = 0.00336 and subsequently increases.

The optimal solutions for the two numerical examples are marked in Tables 3, 4 and 5. The minimum design cost of the material for the case 1 is $7.859C_c$, and for the case 2 is $6.812C_c$.

Fig. 7 shows the input data and the optimal solution for the numerical example (case 1) for the circular isolated footing.

Fig. 8 shows the input data and the optimal solution for the numerical example (case 2) for the circular isolated footing.

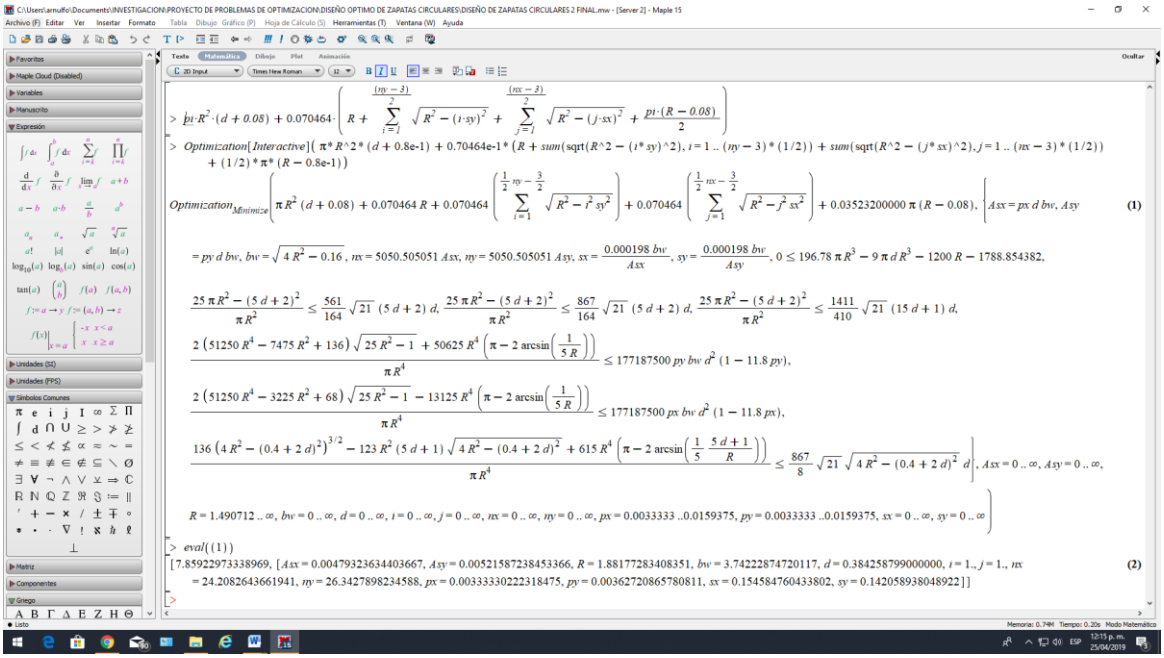

Fig. 7 Input data and the optimal solution (case 1)

Fig. 9 shows the dimensions of the concrete and the steel in general form for the isolated footings of circular shape.

Now, the examples are developed using the procedure for the classical model and proposed model presented by Luévanos-Rojas (2014a). First is proposed the minimum thickness "t" of the footing, which is of 25 cm marking by code ACI, subsequently the thickness is revised to comply the following conditions: moment, bending shear and punching shear. If such conditions are not satisfied is proposed a greater thickness until it fulfills the three conditions mentioned. The thickness that satisfies the three conditions is:

For case 1: the proposed model is of 38.5 cm, and for the classical model is of 57 cm.

For case 2: the proposed model is of 38.5 cm, and for the classical model is of 52 cm.

Table 6 shows the comparison of the classical model and proposed model, and also the comparison of the classical model and optimal design.

The maximum moment $M_{a'\text{-}a'}$ is obtained by the Eq. (5), and the maximum moment $M_{b'\text{-}b'}$ is found by the Eq. (6). The bending shear that resists the concrete $\emptyset_v V_{cf}$ is obtained by the Eq. (45) that is presented in appendix. The bending shear acting V_f is found by the Eq. (7). The punching shear that resists the concrete $\emptyset_v V_{cp}$ is obtained by the Eqs. (48a), (48b) and (48c) that are presented in appendix. The punching shear acting V_p is found by the Eq. (8). The steel area A_{sy} and A_{sx} are obtained by the Eq. (10).

The results show the following (see Table 6):

For the moments that act on the footing: the moments for the classical model are same in the two directions because the pressure diagram is uniform for the two cases. Now the highest percentage is presented with respect to the optimal design for the two cases.

For the bending shear that resists the footing: the highest percentage is presented with respect to the optimal design for the two cases.

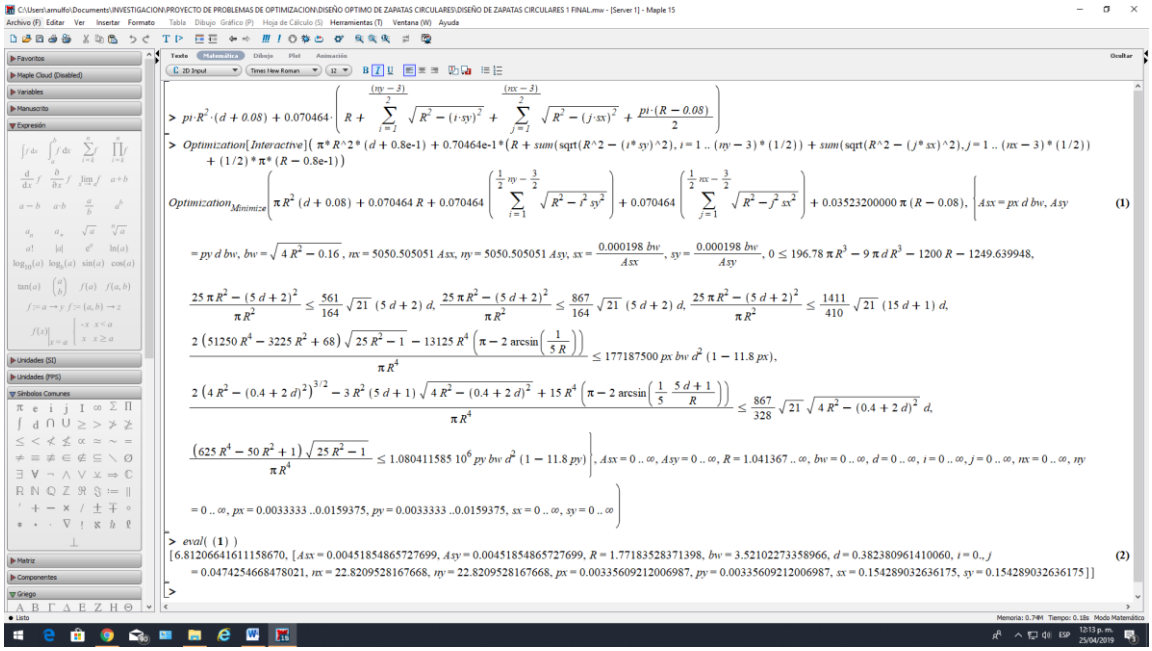

Fig. 8 Input data and the optimal solution (case 2)

For the bending shear that act on the footing: the highest percentage is presented with respect to the optimal design for the two cases.

For the punching shear that resists the footing: the highest percentage is presented with respect to the optimal design for the two cases.

For the punching shear that act on the footing: the highest percentage is presented with respect to the optimal design for the two cases.

For the steel areas of the footing: the steel areas for the classical model are same in the two directions because the pressure diagram is uniform for the two cases. For case 1 is presented the highest percentage with respect to the optimal design. For case 2 the steel areas are equals because the minimum steel governed in the two directions.

For the minimum cost of the footing: the classical model is larger in a 41% with respect to the proposed model, and the classical model is larger in a 44% with respect to the optimal design for the case 1, and for the case 2 the classical model is larger in a 36% with respect to the proposed model, and the classical model is larger in a 44% with respect to the optimal design.

5. Conclusions

The standard design method (classical method) is obtained in the following way: a radius "*R*" is proposed and it must comply with the admissible stress, and then an effective depth or effective cant is found from the maximum moment and compared with the bending shear (unidirectional shear) and the punching shear (bidirectional shear) until it meets these conditions, and then the reinforcing steel is found, but it is not guaranteed that the minimum design cost is obtained.

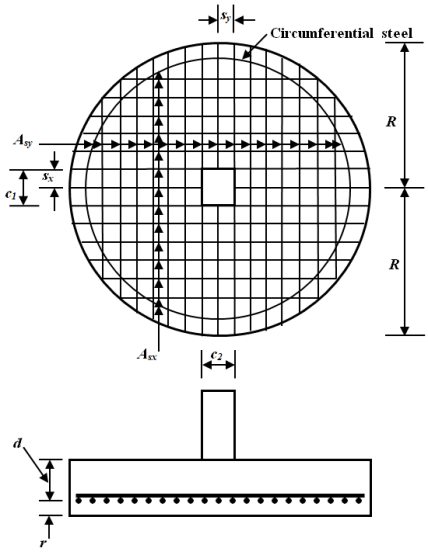

Fig. 9 Circular isolated footing

Table 6 Comparison of results

Concept	Case 1					Case 2				
	CM	PM	OD	CM/PM	CM/OD	CM	PM	OD	CM/PM	CM/OD
$M_{a'\text{-}a'}$ ($kN\text{-}m$)	905.01	731.88	725.08	1.24	1.25	747.71	598.31	597.18	1.25	1.25
$M_{b'\text{-}b'}$ ($kN\text{-}m$)	905.01	620.05	613.59	1.46	1.47	747.71	575.64	574.51	1.30	1.30
D (cm)	380	380	376.36	1.00	1.01	360	355	354.36	1.01	1.02
d (cm)	57	38.5	38.43	1.48	1.48	52	38.5	38.24	1.35	1.36
t (cm)	65	46.5	46.43	1.40	1.40	60	46.5	46.24	1.29	1.30
V_c (m^3)	7.37	5.27	5.17	1.40	1.43	6.11	4.60	4.56	1.33	1.34
$\emptyset_v V_{cf}$ (kN)	1311.22	921.71	910.32	1.42	1.44	1136.12	854.47	847.42	1.33	1.34
V_f (kN)	727.92	713.00	711.90	1.00	1.02	652.72	614.24	615.48	1.06	1.06
$\emptyset_v V_{cp}$ (kN)	4393.45	2401.54	2394.65	1.83	1.83	3801.46	2401.54	2377.24	1.58	1.60
	5631.64	2698.53	2688.91	2.09	2.09	4734.16	2698.53	2664.63	1.75	1.78
	2842.82	1553.94	1549.48	1.83	1.83	2459.77	1553.94	1538.21	1.58	1.60
V_p (kN)	2678.15	1550.89	1549.33	1.73	1.73	2371.80	1537.90	1538.21	1.54	1.54
A_{sy} (cm^2)	71.73	52.52	52.16	1.37	1.38	61.95	45.22	45.19	1.37	1.37
A_{sx} (cm^2)	71.73	48.45	47.93	1.48	1.50	61.95	45.22	45.19	1.37	1.37
C_{tm} ($)	11.28C_c	8.00C_c	7.86C_c	1.41	1.44	9.35C_c	6.86C_c	6.81C_c	1.36	1.37

Where: CM is classical model, PM is the proposed model, OD is the optimal design

The optimal design presented in this document is formulated from an analytical approach based on a minimum cost design criteria and a set of constraints in accordance with the requirements of the construction code for structural concrete and comments (ACI 318S-14 2014). The constant parameters (independent variables) are: c_1, c_2, H, P, M_x, M_y, q_a, γ_c, γ_g, r, α, f'_c y f_y. The decision variables (dependent variables) are: R, d, ρ_y, ρ_x, n_y, n_x, s_y, s_x, A_{sy} and A_{sx}.

The minimum cost design from the optimization technique presented that is lower than the cost obtained from the standard design method (classical method). Furthermore both techniques were verified. This comparison showed the superiority of the optimization technique over the standard design method (classical method).

It can be said that the investigations carried out to find the optimal design of concrete structures are of great value for the practice of engineers. The optimal solution satisfies the provisions of the code and minimizes the cost of the structure.

Using the optimal design, this document successfully acquires a model to predict the proportions of reinforcing steel ρ_y and ρ_x, the optimal areas of steel reinforcement A_{sy} and A_{sx}, the optimum radius of the footing R, the optimum effective depth d and the lowest cost for the reinforced concrete circular isolated footings under to a concentrated load and moments in two generalized directions.

Acknowledgments

The research described in this paper was financially supported by the Institute of Multidisciplinary Researches of the Faculty of Accounting and Administration of the Autonomous University of Coahuila. The authors also gratefully acknowledge the helpful comments and suggestions of the editor and the reviewers, which have improved the presentation.

References

Abbasnia, R., Shayanfar, M. and Khodam, A. (2014), "Reliability-based design optimization of structural systems using a hybrid genetic algorithm", *Struct. Eng. Mech.*, **52**(6), 1099-1120. https://doi.org/10.12989/sem.2014.52.6.1099.

ACI 318S-14 (American Concrete Institute) (2014), Building Code Requirements for Structural Concrete and Commentary, Committee 318.

Aguilera-Mancilla, G., Luévanos-Rojas, A., López-Chavarría, S. and Medina-Elizondo, M. (2019a), "Modeling for the strap combined footings Part I: Optimal dimensioning", *Steel Compos. Struct.,* **32**(2), 97-108. http://dx.doi.org/10.12989/scs.2019.30.2.097.

Al-Ansari, M.S. (2013), "Structural cost of optimized reinforced concrete isolated footing", *Int. Scholarly Scientific Res. Innovation*, **7**(4), 193-200.

Al-Ansari, M.S. (2014), "Cost of reinforced concrete paraboloid shell footing", *J. Struct. Analysis Design*, **1**(3), 111-119.

Aschheim, M., Hernández-Montes, E. and Gil-Martin, L.M. (2008), "Design of optimally reinforced RC beam, column, and wall sections", *J. Struct. Eng.*, **134**(2), 231-239. https://doi.org/10.1061/(ASCE)0733-9445(2008)134:2(231).

Awad Z.K. (2013), "Optimization of a sandwich beam design: analytical and numerical solutions", *Struct. Eng. Mech.*, **48**(1), 93-102. http://dx.doi.org/10.12989/sem.2013.48.1.093.

Bhalchandra, S.A. and Adsul, P.K. (2012), "Cost optimization of doubly reinforced rectangular beam section", *J. Modern Eng. Res.*, **2**(5), 3939-3942.

Bordignon, R. and Kripka, M. (2012), "Optimum design of reinforced concrete columns subjected to uniaxial flexural compression", *Comp. Concrete*, **9**(5), 327-340. http://dx.doi.org/10.12989/cac.2012.9.5.327.

Errouane, H., Deghoul, N., Sereir, Z. and Chateauneuf, A. (2017), "Probability analysis of optimal design for fatigue crack of aluminium plate repaired with bonded composite patch", *Struct. Eng. Mech.*, **61**(3), 325-334. http://dx.doi.org/10.12989/sem.2017.61.3.325.

Fleith de Medeiros, G. and Kripka, M. (2013), "Structural optimization and proposition of pre-sizing parameters for beams in reinforced concrete buildings", *Comp. Concrete*, **11**(3), 253-270. http://dx.doi.org/10.12989/cac.2013.11.3.253.

Gao, Q., Yang, J.D. and Qiao, J.D. (2017), "A multi-parameter optimization technique for prestressed concrete cable-stayed bridges considering prestress in girder", *Struct. Eng. Mech.*, **64**(5), 567-577. http://dx.doi.org/10.12989/sem.2017.64.5.567.

Gharehbaghi, S. (2018). "Damage controlled optimum seismic design of reinforced concrete framed structures", *Struct. Eng. Mech.*, **65**(1), 53-68. http://dx.doi.org/10.12989/sem.2018.65.1.053.

Hwang, Y., Jin, S.S., Jung, H.Y., Kim, S., Lee, J.J. and Jung, H.J. (2018), "Experimental validation of FE model updating based on multi-objective Optimization using the surrogate model", *Struct. Eng. Mech.*, **65**(2), 173-181. http://dx.doi.org/10.12989/sem.2018.65.2.173.

Kao, CH-S. and Yeh, I-CH. (2014a), "Optimal design of reinforced concrete plane frames using artificial neural networks", *Comp. Concrete*, **14**(4), 445-462. http://dx.doi.org/10.12989/cac.2014.14.4.445.

Kao, CH-S. and Yeh, I-CH. (2014b), "Optimal design of plane frame structures using artificial neural networks and ratio variables", *Struct. Eng. Mech.*, **52**(4), 739-753. http://dx.doi.org/10.12989/sem.2014.52.4.739.

Kaveh, A. and Bijari, S. (2018), "Simultaneous analysis, design and Optimization of trusses via force method", *Struct. Eng. Mech.*, **65**(3), 233-241. http://dx.doi.org/10.12989/sem.2018.65.3.233.

Kaveh, A. and Mahdavi, V.R. (2016), "Optimal design of truss structures using a new optimization algorithm based on global sensitivity analysis", *Struct. Eng. Mech.*, **61**(3), 1093-1117. http://dx.doi.org/10.12989/sem.2016.60.6.1093.

Kaveh, A. and Talatahari, S. (2012), "A hybrid CSS and PSO algorithm for optimal design of structures", *Struct. Eng. Mech.*, **42**(6), 783-797. http://dx.doi.org/10.12989/sem.2012.42.6.783.

Kaveh, A., Kalateh-Ahani, M. and Fahimi-Farzam, M. (2013), "Constructability optimal design of reinforced concrete retaining walls using a multi-objective genetic algorithm", *Struct. Eng. Mech.*, **47**(2), 227-245. http://dx.doi.org/10.12989/sem.2013.47.2.227.

Khajehzadeh, M., Taha M.R. and Eslami, M. (2014), "Multi-objective optimization of foundation using global-local gravitational search algorithm", *Struct. Eng. Mech.*, **50**(3), 257-273. http://dx.doi.org/10.12989/sem.2014.50.3.257.

Kripka, M. and Chamberlain Pravia, Z.M. (2013), "Cold-formed steel channel columns optimization with simulated annealing method", *Struct. Eng. Mech.*, **48**(3), 383-394. http://dx.doi.org/10.12989/sem.2013.48.3.383.

López-Chavarría, S., Luévanos-Rojas, A. and Medina-Elizondo, M. (2017a), "A mathematical model for dimensioning of square isolated footings using optimization techniques: general case", *J. Innov. Comput. I.*, **13**(1), 67-74.

López-Chavarría, S., Luévanos-Rojas, A. and Medina-Elizondo, M. (2017b), "Optimal dimensioning for the corner combined footings", *Adv. Comput. Des.*, **2**(2), 169-183. https://doi.org/10.12989/acd.2017.2.2.169.

López-Chavarría, S., Luévanos-Rojas, A. and Medina-Elizondo, M. (2017c), "A new mathematical model for design of square isolated footings for general case", *Int. J. Innov. Comput. I.*, **13**(4), 1149-1168.

Luévanos-Rojas, A. (2012), "A mathematical model for the dimensioning of circular footings", *Far East J. Math. Sci.*, **71**(2), 357-367.

Luévanos-Rojas, A. (2014a), "Design of isolated footings of circular form using a new model", *Struct. Eng. Mech.*, **52**(4), 767-786. http://dx.doi.org/10.12989/sem.2014.52.4.767.

Luévanos-Rojas, A. (2014b), "Design of boundary combined footings of rectangular shape using a new model", *Dyna*, **81**(188), 199-208. http://dx.doi.org/10.15446/dyna.v81n188.41800.

Luévanos-Rojas, A. (2015), "Design of boundary combined footings of trapezoidal form using a new model", *Struct. Eng. Mech.*, **56**(5), 745-765. http://dx.doi.org/10.12989/sem.2015.56.5.745.

Luévanos-Rojas, A. (2016a), "Numerical experimentation for the optimal design of reinforced rectangular concrete beams for singly reinforced sections", *Dyna*, **83**(196), 134-142. http://dx.doi.org/10.15446/dyna.v83n196.48031.

Luévanos-Rojas, A. (2016b), "A comparative study for the design of rectangular and circular isolated footings using new models", *Dyna*, **83**(196), 149-158. http://dx.doi.org/10.15446/dyna.v83n196.51056.

Luévanos-Rojas, A. (2016c), "Un nuevo modelo para diseño de zapatas combinadas rectangulares de lindero con dos lados opuestos restringidos", *Revista Alconpat*, **6**(2), 172-187. http://dx.doi.org/10.21041/ra.v6i2.137.

Luévanos-Rojas, A., Faudoa-Herrera, J.G., Andrade-Vallejo, R.A. and Cano-Alvarez, M.A. (2013), "Design of isolated footings of rectangular form using a new model", *Int. J. Innov. Comput. I.*, **9**(10), 4001-4022.

Luévanos-Rojas, A., López-Chavarría, S. and Medina-Elizondo, M. (2017a), "Optimal design for rectangular isolated footings using the real soil pressure", *Ing. Invest.*, **37**(2), 25-33. http://dx.doi.org/10.15446/ing.investig.v37n2.61447.

Luévanos-Rojas, A., López-Chavarría, S. and Medina-Elizondo, M. (2017b), "A comparative study for design of boundary combined footings of trapezoidal and rectangular forms using new models", *Coupled Syst. Mech.*, **6**(4), 417-437. https://doi.org/10.12989/csm.2017.6.4.417.

Luévanos-Rojas, A., López-Chavarría, S. and Medina-Elizondo, M. (2018a), "Optimización de vigas de concreto reforzado para secciones rectangulares con experimentos numéricos", *Computación y Sistemas*, **22**(2), 599-606. https://doi.org/10.13053/CyS-22-2-2542.

Luévanos-Rojas, A., López-Chavarría, S. and Medina-Elizondo, M. (2018b), "A new model for T-shaped combined footings Part I: Optimal dimensioning", *Geomech. Eng.,* **14**(1), 51-60. https://doi.org/10.12989/gae.2018.14.1.051.

Luévanos-Rojas, A., López-Chavarría, S. and Medina-Elizondo, M. (2018c), "A new model for T-shaped combined footings Part II: Mathematical model for design", *Geomech. Eng.,* **14**(1), 61-69. https://doi.org/10.12989/gae.2018.14.1.061.

Nascimbene, R. (2013), "Analysis and optimal design of fiber-reinforced composite structures: sail against the wind", *Wind Struct.*, **16**(6), 541-560. http://dx.doi.org/10.12989/was.2013.16.6.541.

Ozturk, H.T. and Durmus, A. (2013), "Optimum cost design of RC columns using artificial bee colony algorithm", *Struct. Eng. Mech.*, **45**(5), 643-654. http://dx.doi.org/10.12989/sem.2013.45.5.643.

Rizwan, M., Alam, B., Rehman, F.U., Masud, N., Shahzada, K., Masud, T. (2012), "Cost Optimization of Combined Footings Using Modified Complex Method of Box", *J. Adv. Struct. Geotech. Eng.*, **1**(1), 24-28.

Shayanfar, M.A., Ashoory, M., Bakhshpoori, T. and Farhadi, B. (2013), "Optimization of modal load pattern for pushover analysis of building structures", *Struct. Eng. Mech.*, **47**(1), 119-129. http://dx.doi.org/10.12989/sem.2013.47.1.119.

Tiliouine, B. and Fedghouche, F. (2014), "Cost Optimization of reinforced high strength concrete T-sections in flexure", *Struct. Eng. Mech.*, **49**(1), 65-80. http://dx.doi.org/10.12989/sem.2014.49.1.065.

Velázquez-Santillán, F., Luévanos-Rojas, A., López-Chavarría, S., Medina-Elizondo, M. and Sandoval-Rivas, R. (2018), "Numerical experimentation for the optimal design for reinforced concrete rectangular combined footings", *Adv. Comput. Des.*, **3**(1), 49-69. http://dx.doi.org/10.12989/acd.2018.3.1.049.

Wang, Y., (2009), "Reliability-based economic design optimization of spread foundations", *J. Geotech. Geoenviron.*, **135**(7), 954-959. https://doi.org/10.1061/(ASCE)GT.1943-5606.0000013.

Wang, Y., Kulhawy, F.H. (2008), "Economic design optimization of foundation", *J. Geotech. Geoenviron.*, **134**(8), 1097-1105. https://doi.org/10.1061/(ASCE)1090-0241(2008)134:8(1097).

Yáñez-Palafox, J.A., Luévanos-Rojas, A., López-Chavarría, S. and Medina-Elizondo, M. (2019b), "Modeling for the strap combined footings Part II: Mathematical model for design", *Steel Compos. Struct.,* **32**(2), 109-121. http://dx.doi.org/10.12989/scs.2019.30.2.109.

Yousif, S.T., ALsaffar, I.S., Ahmed, S.M. (2010), "Optimum Design of Singly and Doubly Reinforced Concrete Rectangular Beam Sections: Artificial Neural Networks Application", *Iraqi Journal of Civil Engineering*, **6**(3), 1-19.

Zhang, H.Z., Liu, X., Yi, W.J. and Deng, Y.H. (2018), "Performance comparison of shear walls with openings designed using elastic stress and genetic evolutionary structural Optimization methods", *Struct. Eng. Mech.*, **65**(3), 303-314. http://dx.doi.org/10.12989/sem.2018.65.3.303.

CC

Appendix

Equations for moment in both axes are considered at the face of the column are (ACI 318S-14 2014, Luévanos-Rojas 2016a):

$$M_u = \emptyset_f M_n \tag{35}$$

$$M_u = \emptyset_f b_w d^2 \rho f_y \left(1 - \frac{0.59\rho f_y}{f'_c}\right) \tag{36}$$

$$\rho = \frac{A_s}{bd} \tag{37}$$

$$\rho_b = \frac{0.85\beta_1 f'_c}{f_y}\left(\frac{600}{600 + f_y}\right) \tag{38}$$

$$0.65 \leq \beta_1 = \left(1.05 - \frac{f'_c}{140}\right) \leq 0.85 \tag{39}$$

$$\rho_{máx} = 0.75\rho_b \tag{40}$$

$$\rho_{min} = \begin{cases} \dfrac{0.25\sqrt{f'_c}}{f_y} \\ \dfrac{1.4}{f_y} \end{cases} \tag{41}$$

$$A_{st} = 0.0018 b_w t \tag{42}$$

where: M_u is the factored maximum moment, $\emptyset_f$ is the strength reduction factor by bending and its value is 0.90, b_w is analysis width in structural member, ρ is ratio of A_s (steel area) to bd, β_1 is the factor relating depth of equivalent rectangular compressive stress block to neutral axis depth, f_y is the specified yield strength of reinforcement of steel, f'_c is the specified compressive strength of the concrete at 28 days, A_{st} is the steel area by temperature, t is the total thickness of the footing.

The values of b_{wx} and b_{wy} are the analysis widths for moments on both sides of the column and these are obtained as follows (Luévanos-Rojas 2014a, 2016b):

$$b_{wx} = \sqrt{4R^2 - {c_1}^2};\ b_{wy} = \sqrt{4R^2 - {c_2}^2} \tag{43}$$

Required strength U to resist factored loads or related internal moments and forces is (ACI 318S-14 2014):

$$U = 1.2D + 1.6L \tag{44}$$

where: D is the dead load and L is the live load of the internal moments and forces.

The bending shear (unidirectional shear force) that must resist the concrete provided by the code is obtained by the following equation (ACI 318S-14 2014):

$$\emptyset_v V_{cf} = 0.17\emptyset_v\sqrt{f'_c}b_{wc}d \tag{45}$$

where: V_{cf} is bending shear that must resist the concrete, $\emptyset_v = 0.85$ is the strength reduction factor for the shear, b_{ws} is the analysis width for the bending shear and this is obtained as follows (Luévanos-Rojas, 2014):

$$b_{ws} = \sqrt{4R^2 - (c_1 + 2d)^2} \tag{46}$$

For bending shear that acts on the footing V_f must be compared against the bending shear that must be resisted by the concrete V_{cf}, and this must comply with the following equation (ACI 318S-14 2014):

$$V_f \leq \emptyset_v V_{cf} \tag{47}$$

The punching shear (shear force bidirectional) that must resist the concrete provided by the code is obtained by the following equations (ACI 318S-14 2014):

$$\emptyset_v V_{cp} = 0.17\emptyset_v\left(1 + \frac{2}{\beta_c}\right)\sqrt{f'_c}b_0 d \tag{48a}$$

where: V_{cp} is punching shear that must resist the concrete, β_c is the long side between the short side of the column, b_0 is the perimeter where the punching is presented.

$$\emptyset_v V_{cp} = 0.083\emptyset_v\left(\frac{\alpha_s d}{b_0} + 2\right)\sqrt{f'_c}b_0 d \tag{48b}$$

where: α_s is 20 for corner columns, 30 for edge columns, and 40 for interior columns.

$$\emptyset_v V_{cp} = 0.33\emptyset_v\sqrt{f'_c}b_0 d \tag{48c}$$

Note: $\emptyset_v V_{cp}$ must be the smallest value of Eqs. (48a), (48b) and (48c).

For punching shear that acts on the footing V_p must be compared against the bending shear that must be resisted by the concrete V_{cp}, and this must comply with the following equation (ACI 318S-14 2014):

$$V_p \leq \emptyset_v V_{cp} \tag{49}$$